

Optimising the assignment of swabs and reagents for PCR testing during a viral epidemic

Alberto Santini¹

¹Universitat Pompeu Fabra, Barcelona, Spain — alberto.santini@upf.edu

May 4, 2020

1 Introduction

Viruses are pathogens that replicate after penetrating the living cells of other organisms. Outside cells, a virus is nothing more than genetic material (DNA or RNA) surrounded by protective layers of proteins and lipids. Once inside a host cell, the virus uses the cell's structures to replicate its genetic material and assembly its protective layers, thus creating a copy of itself. At the end, it kills the cell to release both the original and the copy.

Viruses cause a host of human diseases, ranging from the common cold to AIDS. Of particular interest for this work is the recent *Coronavirus disease 2019* (COVID-19) pandemic. Under particular circumstances, a virus (and the disease it causes) can spread to a large part of a population in a short time, leading to an *epidemic*. When the epidemic spreads across national borders and infects people worldwide, it's termed a *pandemic*. SARS-CoV-2, the virus spreading COVID-19, for example, possessed the right characteristics to turn its associated disease into a pandemic: people carrying the virus don't show symptoms for an average of five days, during which they can spread the virus to others [42]; its basic reproduction number has been estimated between 1.4 and 5.7, i.e., each infected person in turns infects an average of up to 5.7 people [31]; up to 44% of patients show no symptoms at all during the infection period, making their diagnosis considerably difficult [27].

A fundamental part of the response put in place to fight epidemics and pandemics is massive testing of the population. When carriers of the virus remain asymptomatic while infecting others, as for COVID-19, testing is one of the main tools health authorities can deploy to contain the spread of the disease [35]. Viruses such as SARS-CoV-2 are RNA viruses, i.e., they contain a single strand of nucleotides rather than the “double helix” typical of DNA. For this brief introduction, we call the four nucleotides composing the RNA chain with their initials: A, C, G, U.

The quickest available test for RNA viruses uses real-time reverse transcription polymerase chain reaction (rRT-PCR). A popular test consists in collecting a sample of nasal secretions on a swab [7], looking for an RNA subsequence which is unique to the virus. To identify this subsequence, the tester uses inverse RNA: a sequence of nucleotides which pairs those they are looking for (remember that A pairs with U and C with G). If the sample contains viral RNA, it will pair with the chain injected by the tester. Once the nucleotides are paired, they effectively transform the single-strand RNA into double-strand DNA. To detect a significant presence of the viral DNA, the genetic material goes through an amplification process, the polymerase chain reaction [6]. Both transforming RNA into DNA, and amplifying it, cannot happen without certain enzymes, commonly called *reagents*. While this simplified description is enough to introduce our problem, we refer the reader to the reviews of Bustin [4] and Freeman, Walker, and Vrana [15] for a more accurate description of the rRT-PCR technique. Figure 1 is an example of a protocol for rRT-PCR tests used by the United Kingdom's National Health Service.

During the COVID-19 pandemic, laboratory capacities and reagent availability have become the bottleneck for increasing the number of tests in much of Europe and North America [12, 1, 41]. Therefore, health authorities

2019-nCoV real-time RT-PCR RdRp gene assay

A. Background

This protocol describes a uniplex real-time RT-PCR assay for the detection of the 2019 novel coronavirus (2019-nCoV). A 100 bp long fragment from a conserved region of the RNA-dependent RNA polymerase (RdRp) gene is detected with FAM labelled hydrolysis probes. The assay will detect 2019-nCoV and SARS virus, as well as other bat-associated SARS-related viruses (Sarbecovirus). In the validated and published format, the assay employs the use of two probes; one will detect 2019-nCoV, SARS-CoV and bat-SARS-related CoVs, and the other 2019-nCoV only.¹ The RdRp gene assay has been evaluated in the Respiratory Virus Unit, PHE, on the ABI 7500 Fast real-time PCR system.

B. Reagents

1. Primers and probes – order from TIB Molbiol, Germany.

Assay	Oligonucleotide ID	Sequence (5' - 3')	Concentration*
RdRp gene	RdRp_SARSr-F2	GTGARATGGTCATGTGTGGCGG	use 600 nM per reaction
	RdRp_SARSr-R1	CARATGTTAAACACATTATGACATA	use 600 nM per reaction
	RdRp_SARSr-P2	FAM-CAGGTGGAACCTCATCAGGAGATGC-BBQ	Specific for 2019-nCoV, will not detect SARS-CoV use 100 nM per reaction and mix with P1
	RdRp_SARSr-P1	FAM-CCAGGTGGWACRTCATCMGGTGATGC-BBQ	Pan Sarbeco-Probe, will detect 2019-nCoV virus, SARS-CoV and bat-SARS-related CoVs use 100 nM per reaction and mix with P2

FAM, 6-carboxyfluorescein; BBQ, blackberry quencher

*Optimized concentrations are mol per liter of final reaction mix.

(e.g., 1.5 microliters of a 10 micromolar (μM) primer stock solution per 25 microliter (μl) total reaction volume yields a final concentration of 600 nanomol per liter (nM) as indicated in the table)

¹Drosten et al. Detection of 2019 novel coronavirus (2019-nCoV) by real-time RT-PCR. Eurosurveillance 2020; 25 (3).

Version 1.0

28.01.2020

2. Invitrogen SuperScript III Platinum one-step qRT-PCR kit. Cat nos. 11732-020 and 11732-088. Order from ThermoFisher Scientific, UK.

C. Preparation of RT-PCR mix and cycling conditions

RdRp-assay

MasterMix:	Single rxn (μl)
H ₂ O (RNase free)	2.1
2x Reaction mix	12.5
MgSO ₄ (50mM)	0.4
RdRp_SARSr-F2 primer (10 μM)	1.5
RdRp_SARSr-R1 primer (10 μM)	2
RdRp_SARSr-P1 probe (10 μM)	0.25
RdRp_SARSr-P2 probe (10 μM)	0.25
SSIII/Taq Enzyme Mix	1
MasterMix per well / total	20
Template RNA	5
	25μl

Cycler:

55°C	10 min	45x cycles
94°C	3 min	
94°C	15 sec	
58°C	30 sec	

Passive reference: none
Standard mode

Figure 1: United Kingdom National Health Service's protocol for rRT-PCR analysis of samples from swabs, to detect COVID-19.

need to optimise the allocation of resources to their test laboratories, starting from the distribution of reagents and the assignments of testing tasks. With this work, we use tools from Operational Research to help decision makers maximise the number of tests they can conduct while limited by reagent availability and logistic constraints.

Our main **contributions** are the following.

- We introduce the problem of maximising a country's test capacity for rRT-PCR tests, during the outbreak of an epidemic. In such a situation, (i) reagent scarcity is often a bottleneck for testing, and (ii) some regions are foci of the disease, requiring more tests than others. These two conditions provide an opportunity to optimise the allocation of reagents and swabs, with the aim of maximising the number of swabs tested and reducing the wait time for results.
- We provide an Integer Programming formulation for this problem, extend it to consider the real-world case in which the health-care system is decentralised at the regional level, and consider a hierarchical multi-objective version of the problem.
- We conduct two case studies to validate our approach. In the first one, we use real-life data referring to the Italian situation during the COVID-19 pandemic. Our analysis confirms that fostering inter-regional collaboration can increase by up to +40% the number of swabs tested during a 13-day planning horizon. In the second one, we use synthetic data to determine the most important factors which impact testing capacity. We conclude that a strong industrial network able to provide a steady supply of reagents provides the greatest advantage, vs. procuring reagents via sporadic shipments, even when the total purchased quantity stays the same. Further, countries with limited lab infrastructure should prioritise acquiring more machines and training more personnel, while increasing inter-regional coordination helps those countries with a developed laboratory network.
- We make available both our data and the code we used, under an open-source license [33].

2 Problem description

In our problem, a set of laboratories $L = \{1, \dots, |L|\}$ has to perform rRT-PCR tests on swabs during a time horizon $T = \{1, \dots, |T|\}$ (each time unit corresponds to a day). We assume, wlog, that for each swab a lab needs one unit of reagent. Each lab $l \in L$ starts with a reserve ρ_{l0} of reagent at the beginning of the time horizon. The labs can receive further units of reagent from factories $R = \{1, \dots, |R|\}$, limited by their production capacity. In this work we are going to assume that each factory $r \in R$ produces f_{rt} units of reagent on day $t \in T$. Factories also store an initial amount ρ_{r0} of reagent at the beginning of the planning horizon. Note that a factory can also model other types of facilities; for example, a warehouse receiving new reagents once per week, or even a one-time shipment from a foreign country.

Each laboratory l has a capacity Q_l of swabs it can test during one day. This capacity applies even if the lab has a larger amount of reagent, due to limitations on available machinery and workforce. The effective testing capacity of l , then, is the minimum between Q_l and the amount of reagent available at l .

A lab $l \in L$ is tasked with testing m_{lt} swabs on day t , according to a predefined schedule to meet epidemiological needs. If a laboratory doesn't have enough reagent to test all the swabs, the decision-maker has three options: (i) moving some reagent from a factory to the lab, (ii) moving some swabs to another lab, or (iii) storing the swabs and schedule their testing for another day.

Remark. We assume the planner has already chosen the laboratory to which they assign the swabs. More generally, though, a planner might need that swabs be tested in a given region, without any constraint on which specific lab performs the test, as long as they are geographically close to the point where the swabs were collected. In [Section 4.1](#), we will extend the model to take into account this general case, making the number of swabs assigned to each lab a decision variable.

The amount of reagent and swabs that a planner can move between locations each day is bounded by q^{rg} and q^{sw} , respectively.

Remark. We assume that quantities q^{rg} and q^{sw} are global capacity limits on the total amount of reagent and swab movements. Such an assumption rests on the observation that, during an epidemic, a central decision-maker manages logistic resources and can reallocate them from one area to another. If this were not the case, it wouldn't be hard to enforce local limits, e.g., on the number of swabs that the planner can move out of a single laboratory. In a model extensions presented in [Section 4.1](#), locations are partitioned in regions and we impose region-specific capacity limits.

Given this input data, a planner must determine, for each day of the planning horizon, (i) how many units of reagent to move from the factories to the laboratories, and (ii) how many swabs to move between laboratories, with the aim of maximising the number of tests carried out.

Remark. While the main objective of the planner is to maximise the number of swabs tested, it's possible to account for secondary objectives. For example, because effective testing must be both large-scale and quick, one might want to minimise the average time swabs spend waiting at lab facilities. In [Section 4.2](#) we propose a multi-objective extension of the problem in which, among all solutions which maximise the number of tests carried out, we select the one with lowest average waiting time.

3 Model formulation

We propose an Integer Programming model using the following sets of variables. The number of units of reagent moved from factory $r \in R$ to lab $l \in L$ on day $t \in T$ is denoted by variable $x_{rlt} \in \mathbb{N}$. Variables $y_{l_1 l_2 t} \in \mathbb{N}$ represents the number of swabs going from laboratory $l_1 \in L$ to $l_2 \in L$ on day $t \in T$. The quantities of reagent stored, respectively, at factory $r \in R$ and lab $l \in L$ on day $t \in T$ are denoted by variables $\rho_{rt} \in \mathbb{N}$ and $\rho_{lt} \in \mathbb{N}$. Variables $z_{lt} \in \mathbb{N}$ represent the number of swabs stored at lab $l \in L$ during day $t \in T$. Laboratories store swabs if they cannot carry out the tests on day t because of a lack of reagents necessary for the rRT-PCR procedure. We assume wlog that, at the beginning of the time horizon, labs don't have any stored swab ($z_{l0} = 0$ for all $l \in L$).

Maximising the number of tests corresponds to minimising the number of swabs stored at labs at the end of the time horizon. The objective function, then, is:

$$\min \sum_{l \in L} z_{l|T}|. \quad (1)$$

The bounds on the quantities of reagent and swabs moved each day translate into the following two constraints:

$$\sum_{r \in R} \sum_{l \in L} x_{rlt} \leq q^{rg} \quad \forall t \in T \quad (2)$$

$$\sum_{l_1 \in L} \sum_{l_2 \in L} y_{l_1 l_2 t} \leq q^{sw} \quad \forall t \in T. \quad (3)$$

The next constraints limit the number of tests carried out at each lab on a given day, based on the quantity of reagent available and lab capacities. To this end, it's convenient to introduce an auxiliary variable $w_{lt} \in \mathbb{N}$ representing the number of tests carried out at lab $l \in L$ on day $t \in T$. Quantities m_{lt} (number of tests requested each day), $\sum_{l' \in L, l' \neq l} y_{l'l t}$ (swabs moving from l to other labs), $\sum_{l' \in L, l' \neq l} y_{ll' t}$ (swabs moving from other labs to l), $z_{l,t-1}$ (swabs backlog from the previous day) and z_{lt} (swabs stored at the end of the day) uniquely determine the value of w_{lt} , according to the linking relation

$$z_{l,t-1} + m_{lt} + \sum_{\substack{l' \in L \\ l' \neq l}} y_{l'l t} = z_{lt} + w_{lt} + \sum_{\substack{l' \in L \\ l' \neq l}} y_{ll' t} \quad \forall l \in L, \forall t \in T. \quad (4)$$

Figure 2 shows this relation visually. In the figure, each node represents lab l on a different day and arrows display the flow of swabs in and out of the laboratory.

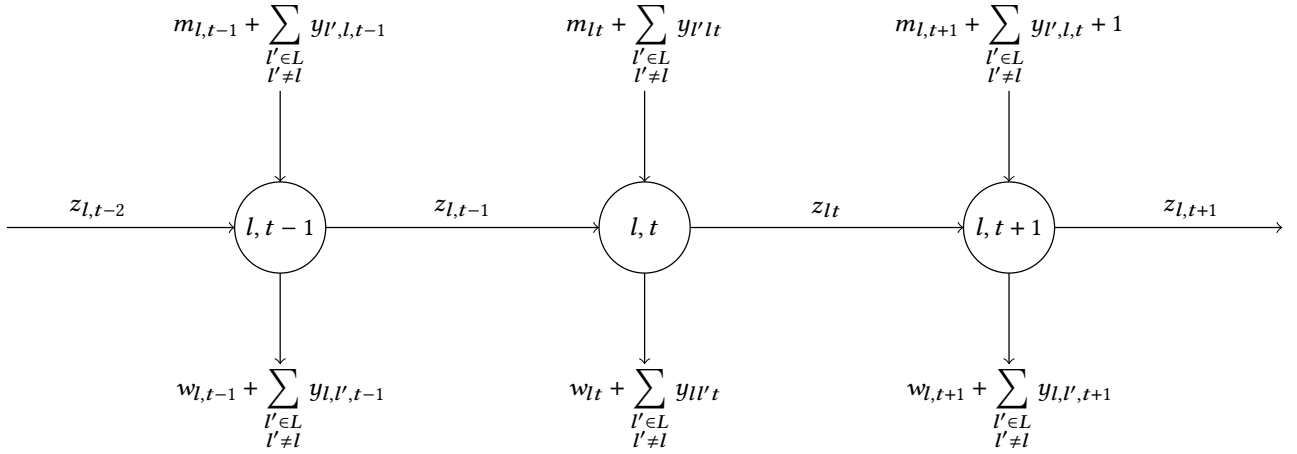


Figure 2: Linking relation between parameter m and variables y , z and w for a lab $l \in L$ at time intervals from $t - 1$ to $t + 1$.

With linking variables w_{lt} , we can constrain the number of tests performed with the following inequalities:

$$w_{lt} \leq \rho_{l,t-1} + \sum_{r \in R} x_{rlt} \quad \forall l \in L, \forall t \in T \quad (5)$$

$$w_{lt} \leq Q_l \quad \forall l \in L, \forall t \in T. \quad (6)$$

Next, we consider flow balance equations analogous to eq. (4), relative to the number of reagent stored at factories and laboratories:

$$\rho_{r,t-1} + f_{rt} = \rho_{rt} + \sum_{l \in L} x_{rlt} \quad \forall r \in R, \forall t \in T \quad (7)$$

$$\rho_{l,t-1} + \sum_{r \in R} x_{rlt} = \rho_{lt} + w_{lt} \quad \forall l \in L, \forall t \in T. \quad (8)$$

Constraint (7) states that the quantity of reagent in the factory's inventory at the beginning of the day, plus the quantity produced, is equal to the quantity in inventory at the end of the day, plus the quantity shipped to the labs. Constraint (8) equates, on the left-hand side, the quantity of reagent in the lab's inventory at the start of the day and the total amount received with, on the right-hand side, the inventory at the end of the day, plus the quantity of reagent used (or, which is the same, the number of tests performed). Note that, because all variables are non-negative, constraint (8) makes constraint (5) redundant.

Model (1)–(8), together with the following variable domain definitions, is the **Base Model** for our problem.

$$x_{r,t} \in \mathbb{N} \quad \forall r \in R, \forall l \in L, \forall t \in T \quad (9)$$

$$y_{l_1 l_2 t} \in \mathbb{N} \quad \forall l_1 \in L, \forall l_2 \in L \setminus \{l_1\}, \forall t \in T \quad (10)$$

$$\rho_{rt} \in \mathbb{N} \quad \forall r \in R, \forall t \in T \quad (11)$$

$$\rho_{lt}, z_{lt}, w_{lt} \in \mathbb{N} \quad \forall l \in L, \forall t \in T \quad (12)$$

3.1 Model strengthening

A disadvantage of the *Base Model* (1)–(12) is that it suffers from symmetry. For example, consider any solution with slack capacity to transport swabs between two labs $l_1, l_2 \in L$ during a day $t \in T$. One can get another solution of the same cost in which, on day t , l_1 sends one more swab to l_2 and l_2 sends one more swab to l_1 . To reduce symmetry, we impose two restrictions on the transport of swabs between labs: (i) a lab l can ship out swabs only if it's already working at full capacity, i.e., it's testing Q_l swabs or it ran out of reagent; (ii) a lab can only send or receive swabs during a given day, but not both.

To tackle the first restriction, we introduce indicator variables $\gamma_{lt} \in \{0, 1\}$, which take value 1 iff lab $l \in L$ is running at full capacity during day $t \in T$. These variables link to variables w and ρ via the following *indicator constraints* (see, e.g., [3]):

$$\gamma_{lt} = 0 \rightarrow w_{lt} \leq Q_l - 1 \quad \forall l \in L, \forall t \in T \quad (13)$$

$$\gamma_{lt} = 0 \rightarrow \rho_{lt} \geq 1 \quad \forall l \in L, \forall t \in T \quad (14)$$

$$\gamma_{lt} = 1 \rightarrow (w_{lt} = Q_l) \vee (\rho_{lt} = 0) \quad \forall l \in L, \forall t \in T. \quad (15)$$

The restriction is, then, enforced with another indicator constraint:

$$\gamma_{lt} = 0 \rightarrow \sum_{\substack{l' \in L \\ l' \neq l}} y_{ll't} = 0 \quad \forall l \in L, t \in T. \quad (16)$$

Constraint (16) guarantees that laboratory l cannot ship out swabs unless it's at full capacity.

To address the second restriction, we can add two more sets of indicator variables and constraints, keeping track of whether a lab sends out or receives swabs. Note that the black-box commercial solver we use (Gurobi) converts all indicator constraints presented in this section into linear constraints. The new variables are $\gamma_{lt}^+, \gamma_{lt}^- \in \{0, 1\}$, which assume value 1 iff, respectively, lab l sends or receives swabs on day t . The necessary constraints to link these variables and enforce the restriction are:

$$\gamma_{lt}^+ = 1 \rightarrow \sum_{\substack{l' \in L \\ l' \neq l}} y_{ll't} \geq 1, \quad \gamma_{lt}^+ = 0 \rightarrow \sum_{\substack{l' \in L \\ l' \neq l}} y_{ll't} = 0 \quad \forall l \in L, \forall t \in T \quad (17)$$

$$\gamma_{lt}^- = 1 \rightarrow \sum_{\substack{l' \in L \\ l' \neq l}} y_{l'l t} \geq 1, \quad \gamma_{lt}^- = 0 \rightarrow \sum_{\substack{l' \in L \\ l' \neq l}} y_{l'l t} = 0 \quad \forall l \in L, \forall t \in T \quad (18)$$

$$\gamma_{lt}^+ + \gamma_{lt}^- \leq 1 \quad \forall l \in L, \forall t \in T. \quad (19)$$

Constraint (19) enforces that each lab, on each day, cannot both send and receive swabs. Note that this restriction also avoids that a laboratory works as a relay, sending and re-shipping swabs between otherwise distant labs.

4 Model extensions

In this section we propose extensions to the model presented above, to account for more realistic scenarios.

4.1 Regional partitioning

In [Section 2](#) we mentioned two limitations of the *Base Model* which might not hold true in real-life applications. The first limitation is that there is a fixed quantity of swabs assigned to each laboratory. In most countries, central or regional health authorities oversee and plan testing. Swabs collected in a region, for example, might be sent for testing to any laboratory in the same region. The second limitation is that tests (and reagents) can move overnight from any location to any other location subject to global capacity limits. When applying the model to large countries, though, logistic constraints might impose that movement of material only happen between geographically close locations.

To address these aspects, we extend the initial problem formulation as follows. The set of laboratories is partitioned as $L = L_1 \cup \dots \cup L_n$ (with $L_i \cap L_j = \emptyset$ for any two $i, j \in \{1, \dots, n\}$, $i \neq j$). We call each set composing the partition a *region*.

The planner receives as input the number of swabs to test each day in each region L_i , denoted as m_{it} , but must determine how to split the swabs between the region's labs. A parameter $\delta_{rl} \in \{0, 1\}$ determines whether a factory $r \in R$ can ship reagent overnight to laboratory $l \in L$. Analogously, parameter $\mu_{l_1 l_2} \in \{0, 1\}$ determines whether two labs $l_1, l_2 \in L$ can send each other swabs overnight.

In our model, logistic capacities refer to each region. We consider, respectively, quantities q_i^{rg} and q_i^{sw} of reagent and swabs that can be shipped to region $i \in \{1, \dots, n\}$ in a day. Depending on the logistic infrastructure, a planner could specify bounds at different levels of aggregation and for both inbound and outbound movements. For example, one might consider a maximum number of reagents shipped out of a factory, or a group of factories. Although we present here regional-level inbound capacities, our formulation is flexible enough to allow a wide array of modelling options. We present an **Extended Model**, taking into account the above considerations, in [Appendix A](#).

4.2 Multi-objective model

As discussed in [Section 2](#), the number of tests carried out is not the only important parameter for an effective testing campaign. Having fast results also helps assessing the disease's spread and enact appropriate and well-timed confinement and mitigation measures.

We propose, then, a Multi-Objective Optimisation (MOO) approach to the problem. For a recent review of MOO applications in optimisation, we refer the reader to Gunantara [16] and Kalyanmoy [19]. In the following, we consider the hierarchical objective approach, in which the planner first optimises for their main objective (number of tests performed) and then, among all the solutions which give an optimal objective value, looks for the one optimising a secondary objective (mean test waiting time).

Let Z^* be the optimal objective value of model (22)–(43). We can obtain the solution to the hierarchical problem by solving the following **Hierarchical Model**:

$$\min \sum_{l \in L} \sum_{t \in T} z_{lt} \quad (20)$$

$$\text{s.t. } \sum_{l \in L} z_{l|T|} = Z^* \quad (21)$$

$$(23)–(43),$$

where [eq. \(20\)](#) minimises the sum of all amounts of swabs stored at labs waiting to be tested and [eq. \(21\)](#) imposes that the considered solutions match the optimal value with respect to objective function (22). Objective function (20) is equivalent to minimising the average swab waiting time because (21) fixes the total number of swabs tested. Note that, when minimising the primary objective, two untested swabs collected, respectively, on the first and last day of the time horizon would contribute the same penalty. Adding the

secondary objective avoids solution where old swabs remain untested for a long time, while newer ones get tested quickly.

5 Related work

Our problem, described in [Section 2](#), resembles superficially problems in the area of production planning, material requirement planning and supply chain optimisation (for a complete overview on these topics see, e.g., Pochet and Wolsey [28]). In our case, carrying out tests corresponds to manufacturing a product using two raw materials (swabs and reagents); for us, though, the finished product demand (tested swabs) always matches one of the raw materials' availability (swabs), while the other (reagents) acts as a bottleneck for production. As in production planning, we deal with the flow of goods over time, including shipments of raw material and inventory carry-over. We also allow the creation of backlogs, i.e., the storage of swabs which cannot be tested on the day of collection. Other characteristics of our problem, however, aren't frequently considered in production planning optimisation: the geographic position of suppliers and production facilities (in our case, laboratories) and their regional subdivision; the possibility of reassigning orders between facilities, subject to logistics constraints; the uneven demand between regions.

Most importantly, unlike problems in production planning, we disregard costs and focus exclusively on maximising production (in our case, number of tests). To this end, we don't consider transport, production, storage, raw material, order placement, personnel, nor opportunity costs, which instead have a prominent role when optimising commercial supply chains and production processes. In the standard case, in fact, the aim of the planner is pure cost minimisation [28] and satisfying the demand in full could even be sub-optimal, if the cost of producing one more unit is larger than the opportunity cost of missing a sale. Other approaches commonly used in production planning include multi-objective optimisation in which cost minimisation is tackled together with secondary objectives, such as demand satisfaction [25], steadiness of production rates [38] or environmental performance [2]. Even in the healthcare sector, if considering times when authorities are not responding to an emergency, costs are taken into account. For example, Zhao et al. [46] consider a drugs production planning problem in which they minimise both costs (avoiding over-production of drugs) and the duration of the trial. Other works (e.g., [10, 13]) have considered the production and supply optimisation problems in the clinical area, but have focused on production and distribution of drugs in "normal" times, rather than during an emergency response to a sudden epidemic event.

Literature focusing specifically on allocation of medical resources during emergencies mainly concentrates on the distribution of (life-saving) medical devices. As such, most models optimise the assignment of existing material to hospitals or individual patients, rather than the production and allocation of new material. Xiang and Zhuang [44], for example, consider the problem of assigning medical resources to patients, taking into account that the conditions of patients left untreated will deteriorate over time. Cao and Huang [5] use a simulation approach in which they consider different strategies to allocate scarce medical resources (e.g., milder patients first, critical patients first, randomly) and complement an analysis of the utility of each strategy with ethical considerations on prioritising some patients over others.

In the wake of the COVID-19 epidemics, the optimisation community has rushed to provide decision support tools for decision-makers involved in the fight against the virus. Similar to our work, researchers at MIT's Operations Research Center [9, 8] have shown the advantages of inter-regional collaboration in sharing automatic ventilators across U.S. states. Mehrotra et al. [22] consider the same problem and use a stochastic model to show how sharing ventilators across states, even when each state is averse to the risk of not having enough machines for its own patients, can reduce the probability of shortages. The problem of allocating ventilator during influenza epidemics was already considered in the literature, e.g., by Huang et al. [18], Meltzer et al. [23], and Zaza et al. [45].

Lampariello and Sagratella [21] study a problem that, like ours, concerns diagnostic tests during the COVID-19 pandemics. The authors consider the problem of deciding how many swabs each region should collect to provide an accurate estimate of the prevalence of the disease among its population, while restricted by a nation-wide capacity limit on the number of tests performed. The problem is motivated by the practice employed in Italy during the early period of the epidemic, of double-checking at one single central laboratory

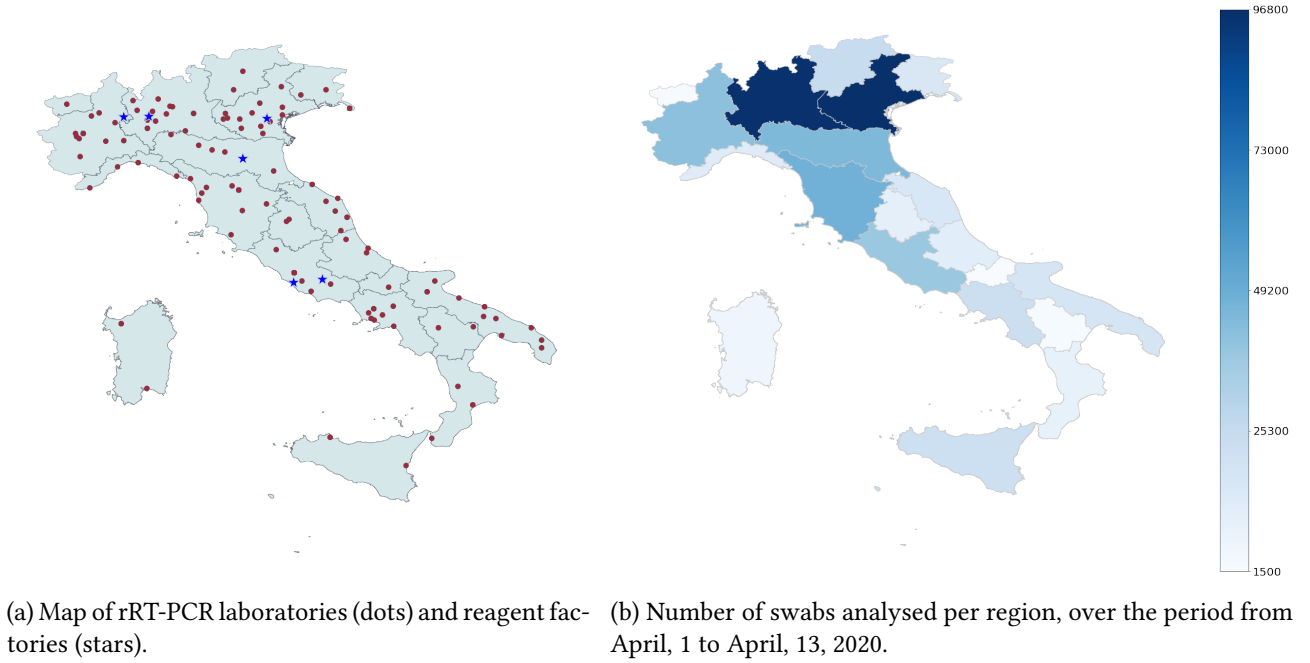


Figure 3: Regional-level data for Italy.

(located in Rome) the results of each positive test conducted by local labs. The capacity of the central lab limits, in this case, the number of total expected positive results coming from all other labs in the country. Note how a decision maker working under the assumptions of [21] can use the model therein to generate regional demands m_{it} , which they can then feed to our model.

Finally, Seccia [34] considers the problem of devising balanced rosters for nurses in hospitals while, due to the virus outbreak, there is both a peak in demand for nurses' services and fewer available health professionals, because many are COVID-19-positive and confined at home.

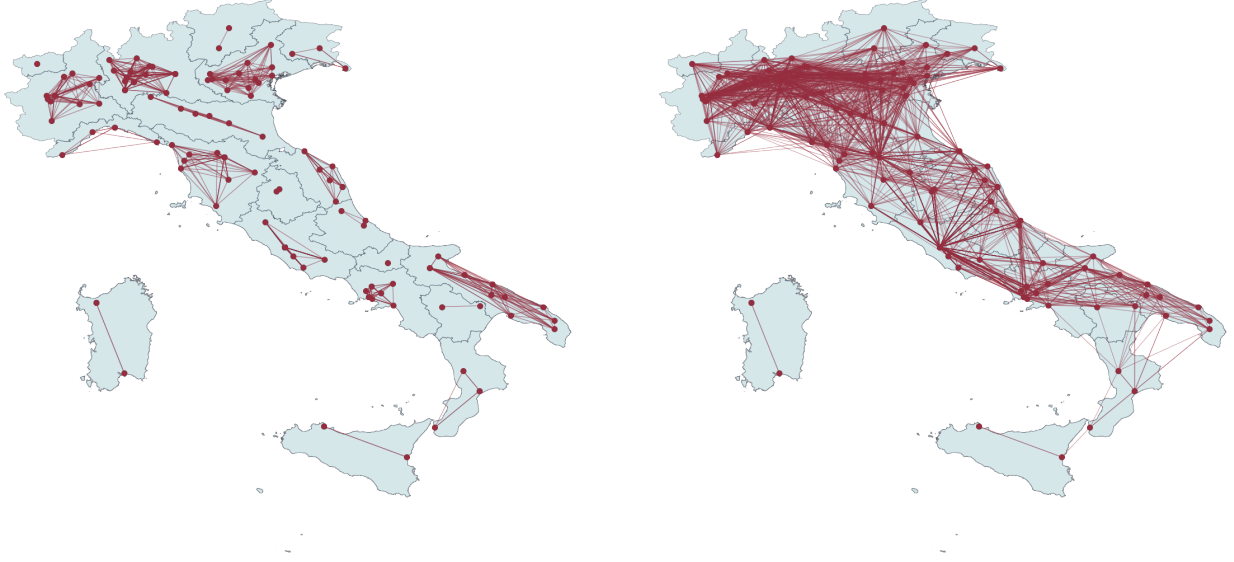
6 Computational analysis

We want to assess the impact of optimising the allocation of reagents and swabs to laboratories on the testing capacity of a country. We present two case studies. In the first, we perform an analysis on a realistic dataset relative to the Italian response to the COVID-19 pandemic, during the period from April 1st to April 13th, 2020. In the second, we use synthetic data to do a sensitivity analysis highlighting the decisions a planner can take to most increase testing capacity and lower waiting times. The datasets and the code used are available at Santini [33]. We use the Hierarchical Model, which we solve using commercial solver Gurobi [17] with a time limit of 15 minutes for the primary and 5 minutes for the secondary objective, on a laptop equipped with a 4-core Intel i7 processor running at 1.6GHz.

6.1 Italy, April 1–13, 2020

We create a set of instances based on data sources relative to the COVID-19 pandemic in Italy [30, 24, 26, 36, 11]. We use data for the period 01–13 April, 2020 for the entire national territory. Figure 3a shows the distribution of laboratories and reagent factories in Italy [24]: dots represents labs which are officially authorised to execute COVID-19 swab tests by the Italian Health Ministry, while stars represent factories whose testing kits (including reagents, extraction kits, probes, negative controls) have been certified for use in COVID-19 swab testing. Figure 3b reports the number of swabs analysed in Italy during the period 01–13 April, 2020, on a regional basis. We note that there is no publicly available data on the average wait times between swab collection and analysis.

We analyse the number of swabs tested, day by day and region by region, using five different scenarios. The first uses the official numbers released by Italy's "Dipartimento della Protezione Civile", which we refer to as



(a) Swabs can only be transported between labs in the same region. (b) Laboratories in the same region or within 200Km can send swabs.

Figure 4: Map of testing laboratories in Italy. An edge connects two laboratories if they can send swabs between each other overnight.

Real Data. Next, we consider the output obtained by the Hierarchical Model, under the following hypotheses. Swabs collected in a region cannot be sent to other regions, but can be allocated to any laboratory within the collection region (for this reason we label this data as **Model - Regional**). In modelling terms, this corresponds to setting $\mu_{l_1 l_2} = 1$ if and only if, for two labs $l_1, l_2 \in L$, there is a region L_k such that $l_1, l_2 \in L_k$. We use this hypothesis to model how testing happens in Italy, with local laboratories and regional “reference laboratories” collecting swabs from all-over the region and providing double checks before non-urgent hospital admissions (emergency patients are admitted even before test results are ready) and discharges. Also remind that the Italian healthcare system is managed on a regional basis, with ample autonomy given to the local health authorities but little inter-regional interaction [14]. We assume that labs can procure reagents from their geographically closest factory, and that procurement is optimised in a centralised way, with the planner deciding the quantities of reagent sent to each laboratory, to maximise the number of tested swabs. Because news sources and press releases by regional health authorities (we found statements by authorities of Basilicata, Campania, Emilia-Romagna, Marche, Lombardia, Piemonte, Puglia, Sardegna, Sicilia, Toscana, Umbria and Veneto, i.e., 12 out of the 20 Italian regions) hint that reagents were a major bottleneck in expanding test capabilities, we expect this model to be able to increase the number of swabs tested even if it doesn’t allow inter-regional swab reassignment, just by optimising reagents assignment. Figure 4a shows how laboratories cluster within each region: an edge between two laboratories means that they belong to the same region.

Finally, we consider the output obtained from the Hierarchical Model, but allowing for reallocation of swabs between laboratories in different regions. This assumption effectively means that regional daily demand can be shared across regions. Because swabs would need to move within a short time (e.g., overnight) we put limitations on the inter-laboratory distance that allows swab transfer. We consider three thresholds of 100Km, 200Km and 400Km and we denote the corresponding data as **Model - 100Km**, **Model - 200Km** and **Model - 400Km**. (We make an exception for the island region of Sardinia, for which moving swabs outside of the region would be unfeasible even if there are other laboratories within 400Km.) Figure 4b shows how laboratories can transfer swabs when using the 200Km threshold. Compare Figures 4a and 4b to note how inter-regional collaboration gives a central planner more opportunities to move swabs between regions in case there should be a day with a demand peak in a particular area. We refer the reader to [33] for the full description of the instance generation process and to [32] for an interactive dashboard presenting the results of the analysis.

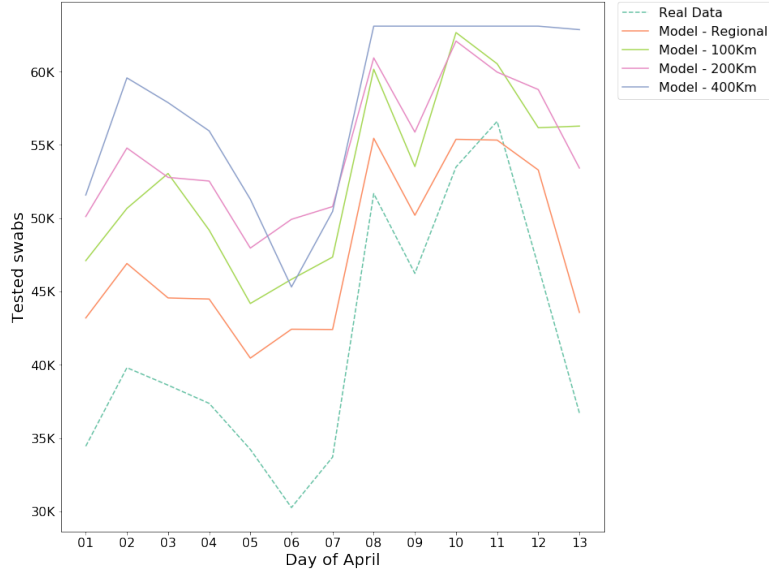


Figure 5: Number of swab tests performed on the national territory, per day. The dashed line reports official numbers from the Civil Defence agency. The other lines represent the results from applying the *Hierarchical Model* with intra-regional (orange column) and inter-regional (green, pink and blue lines) swab transfers. line inter-regional transfer radii considered are 100, 200 and 400Km.

Day of April	Real Data #tests	Model - Regional #tests %gain	Model - 100Km #tests %gain	Model - 200Km #tests %gain	Model - 400Km #tests %gain
1	34455	43202 25.39	47110 36.73	47110 36.73	47110 36.73
2	39809	46916 17.85	50674 27.29	50674 27.29	50674 27.29
3	38617	44567 15.41	53055 37.39	53055 37.39	53055 37.39
4	37375	44492 19.04	49190 31.61	49190 31.61	49190 31.61
5	34237	40463 18.19	44187 29.06	44187 29.06	44187 29.06
6	30271	42433 40.18	45835 51.42	45835 51.42	45835 51.42
7	33713	42414 25.81	47353 40.46	47353 40.46	47353 40.46
8	51680	55454 7.30	60163 16.41	60163 16.41	60163 16.41
9	46244	50207 8.57	53528 15.75	53528 15.75	53528 15.75
10	53495	55385 3.53	62666 17.14	62666 17.14	62666 17.14
11	56609	55332 -2.26	60536 6.94	60536 6.94	60536 6.94
12	46720	53292 14.07	56175 20.24	56175 20.24	56175 20.24
13	36717	43582 18.70	56287 53.30	56287 53.30	56287 53.30
Total	539942	617739 14.41	686759 27.19	709996 31.49	750464 38.99

Table 1: Number of swabs tested on the national territory, day by day, from official real data and from the results obtained using our model. Columns *#tests* represent the number of swabs tested each day. Columns *%gain* are the percentage gains obtained using the model, compared to the real data.

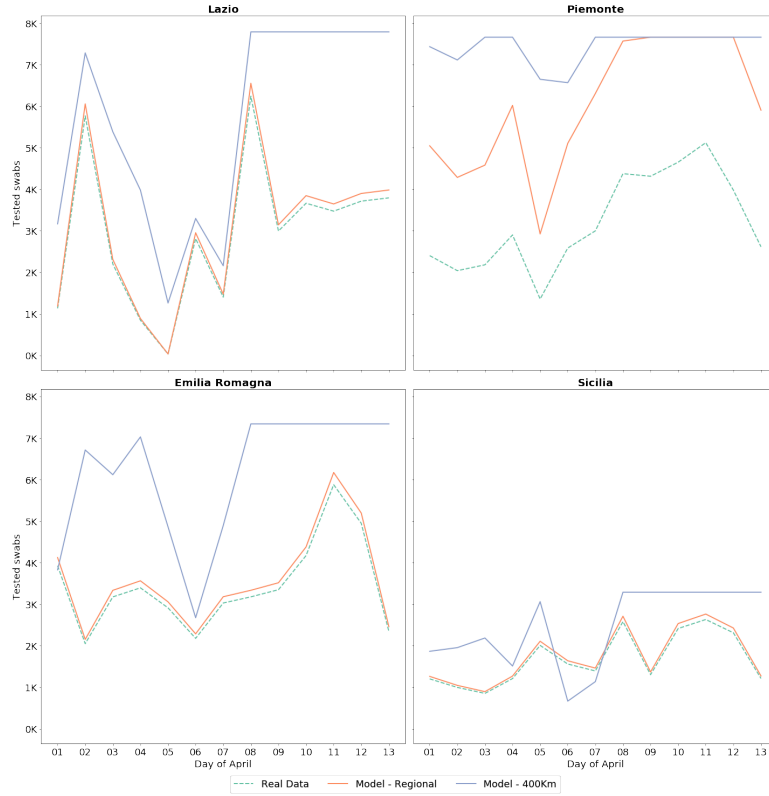


Figure 6: Number of swab tests performed in four Italian regions. The dashed line reports official numbers from the Civil Defence agency. The solid lines represents results obtained with our *Hierarchical Model* allowing intra-regional (orange line) and inter-regional (blue line) swab transfers.

Figure 5 shows the number of swabs tested, day-by-day, when using our proposed models *Regional*, *100Km*, *200Km*, and *400Km*. Note how *Model - 400Km* fully uses the system’s capacity during the last period of the time horizon, where the number of tested swabs becomes a flat line. During some days, a model with fewer lab transfer capabilities gives more tested swabs than a model in which more transfers are allowed. For example, on April 6, using *Model - 400Km* results in fewer tests than *Model - 200Km* and *Model - 100Km*. This is not surprising if we consider that the models maximise the number of swabs tested over the whole planning horizon, even if this results in fewer tests on any particular day.

Table 1 reports detailed results of the analysis. Each row corresponds to one day, and the columns list the real data and the results obtained using the model. Columns *#tests* report the number of swabs tested during that day. Columns *%gain* are the percentage gains obtained using the models, compared to the number of swabs actually tested in Italy in the described period. The last row gives aggregate results for the whole country. Note how using optimisation techniques results in a testing capacity increase between 14% and 39%, under the hypotheses explained above. In particular, assuming that tests in Italy were largely limited by the unavailability of reagents due to a poor allocation of supplies and low inter-regional collaboration, optimising these two aspects can allow to perform up to 250 000 more tests (the increase between *Real Data* and *Model - 400Km*) during 13 days.

Figure 6 shows example results from the *Regional* and *400Km* models, for four representative Italian regions from the north (Piemonte and Emilia-Romagna), the centre (Lazio) and the south (Sicilia) of the country. Each chart reports the number of swabs analysed per day. In these regions, during the last period of the planning horizon, the models use the full laboratory capacity and their curves appear flat, i.e., the limiting factor isn’t reagent availability anymore, but structural limitations such as testing machines or lab personnel. Note how, in Sicily during the middle period, the *400Km* model provides a solution with fewer tested swabs than the *Regional* model and the *Real Data*, for two days. However, there was a catch-up on the tests during the last part of the planning horizon, resulting in more tests carried out in total.

6.2 Synthetic data

By conducting a scenario analysis on synthetic data, we want to learn how some aspects of the healthcare system of the area hit by an epidemic can affect its ability to perform large-scale testing of the population. The factors we analyse are:

1. The effects of having a healthcare system with a large level of independent decision-making at the sub-national level (as is the case, e.g., of Italian regions, Spanish autonomous communities, German lander or the United States) and the benefits of increased cross-regional collaboration, common planning, and resource sharing.
2. The capillarity and production capacity of bio-chemical and pharmaceutical industries able to prepare the reagents needed to carry out rRT-PCR tests, especially in light of the increasing trend to off-shore such manufacturing capabilities to developing countries (see, e.g., [20, 40]).
3. Reagent-independent laboratory capacity, i.e., the test capacity deriving by the number of available machines and personnel. This corresponds to the full laboratory capacity in the ideal case in which any amount of reagents were immediately available.
4. The logistic capabilities of the country, i.e., how labs can procure reagents from manufacturing facilities and transfer swabs away from saturated labs.

6.2.1 Instance generation

We list in the following the characteristics of the instances we generate. We consider $|L| = 100$ laboratories, which we distribute in the square $S = [0, 100]^2$ in the euclidean plane as explained below. First, we define parameter $\lambda_{L \times R}$, which is the expected size of regions, i.e., the expected number of labs in each region. Next, we select $n = \lfloor |L| / \lambda_{L \times R} \rfloor$ random points in $[10, 90]^2$ which we use as initial centroids for the regions (note how we excluded the external boundary of S). We place the labs in S by first choosing a random centroid and then a random point in S which lies at distance of at most 20 from the centroid, and repeating this procedure $|L|$ times. In this way, we aim at placing clusters in loose regional clusters. To complete the assignment of labs to regions, we assign each lab to its closest centroid.

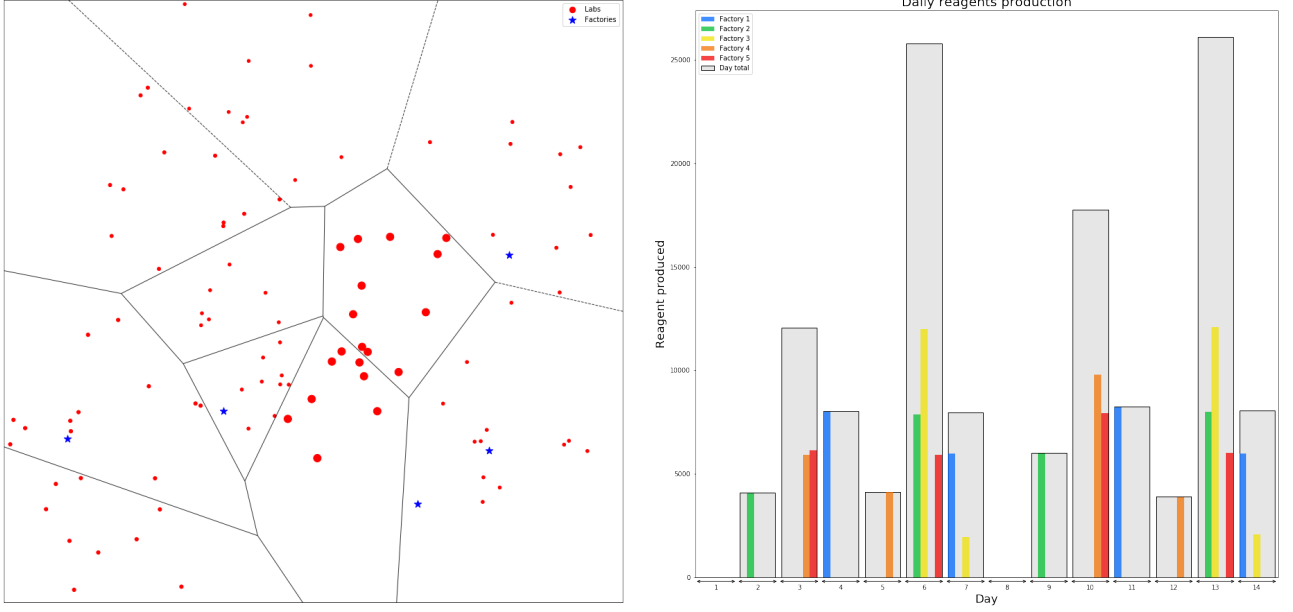
Another parameter, $\lambda_{F \times R}$, determines how distributed is the country's reagent production capacity; this parameter represents the expected number of reagent factories per region. We place $|R| = n \cdot \lambda_{F \times R}$ factories at random in S . Figure 7a shows an example distribution of labs and factories. Dots represent laboratories, stars denote factories, and lines are the Voronoi boundaries (see, e.g., [29, Ch. 5]) associated with regional centroids (i.e., the lines delimit the regions).

To determine the demand of each region, we assume that 40% of the regions will have a criticality, such as a focus of the illness, and will thus require more tests. (For example, during the COVID-19 pandemics, the Chinese province of Wuhan, northern Italian regions, the autonomous communities of La Rioja, Madrid and Castilla-La Mancha in Spain, or the states of Washington and New York in the U.S.A. were foci in their respective countries.) The other regions might, instead, have some spare capacity which they can use, if resources are properly coordinated, to help saturated regions. Let $\bar{m} = 100$ be an ideal number of tests to perform per lab per day (assuming ideal conditions), and let $|L_i|$ be the number of labs in region i . The number of tests requested in region i on day t is

$$m_{it} = \begin{cases} \bar{m} \cdot |L_i| \cdot 2 \cdot \varepsilon & \text{for 40\% randomly chosen regions} \\ \bar{m} \cdot |L_i| \cdot 0.75 \cdot \varepsilon & \text{for the remaining 60\% of regions,} \end{cases}$$

where ε is a noise term distributed according to a truncated normal distribution between 0.95 and 1.05. The definition of m_{it} is justified by the assumption that the number of swabs to test depends on regional population, which correlates positively with the number of laboratories in the region. The dot size in Figure 7a is directly proportional to the lab's region average demand in the example instance; note how two bordering regions are "critical".

Lab capacities are then defined as a fraction of the ideal number of tests assigned to each lab: $Q_l = \bar{m} \lambda_{LC}$, where λ_{LC} is a parameter. Values of the parameter larger than 1 correspond to a situation in which reagent



(a) Spatial set-up of the instance. Dots represent laboratories, with their size proportional to the average daily demand in their region. Stars represent factories and lines are regional boundaries. (b) Daily reagent production. Each smaller bar represents one factory and the larger bars represent the total daily production.

Figure 7: Example of a synthetic instance with *bumpy* reagent production at factories.

availability is the main bottleneck for testing, while smaller values indicate that laboratories have structural deficiencies which limit the number of swabs they can test, even when reagents are abundant. Each lab can procure reagents from its λ_{LF} closest factories, and can send swabs to other laboratories in the same region. A parameter λ_{LL} gives the maximum distance at which two labs in different regions can exchange swabs. In particular, when $\lambda_{LL} = 0$ we forbid cross-regional collaboration and sharing of testing capacity.

Regional inbound capacities for reagents (q_i^{rg}) and for swabs (q_i^{sw}) are determined as:

$$q_i^{\text{rg}} = \begin{cases} \bar{m} \cdot |L_i| & \text{for 80\% of the regions} \\ \bar{m} \cdot |L_i| \cdot 0.75 & \text{for 20\% "impervious" regions} \end{cases} \quad q_i^{\text{sw}} = \begin{cases} \bar{m} \cdot |L_i| \cdot 0.25 & \text{for 80\% of the regions} \\ \bar{m} \cdot |L_i| \cdot 0.10 & \text{for 20\% "impervious" regions,} \end{cases}$$

We assume here that the “impervious” regions have tighter logistical constraints; for example, islands, mountainous areas, or regions with poorer infrastructure. We set the initial amount of reagent stored at labs and factories to a minimal amount, as follows:

$$\rho_{l0} = \bar{m} \cdot \varepsilon \quad \rho_{r0} = \bar{m} \cdot \frac{\lambda_{L \times R}}{\lambda_{F \times R}} \cdot \varepsilon,$$

where ε is distributed according to a truncated normal distribution between 0 and 0.25. Such a choice corresponds to labs and factories having a small fraction of their daily, respectively needed and produced, reagents in the initial stock – a situation that can commonly occur during an epidemic, when safety stocks are quickly depleted.

Last, we describe how we determine factories’ daily production. We propose two production patterns (selected via parameter λ_{pp}): steady and bumpy. Under the steady pattern, each factory r produces $f_{rt} = \bar{m} \cdot \frac{\lambda_{L \times R}}{\lambda_{F \times R}} \cdot \lambda_{\text{FP}} \cdot \varepsilon$ units of reagent each day, where ε follows a truncated normal distribution between 0.95 and 1.05 and λ_{FP} is a parameter. Note how $\lambda_{\text{FP}} < 1$ drives the total factory production capacity to be smaller than the total demand, indicating a situation in which there are fewer reagents than the nation needs. Values of $\lambda_{\text{FP}} \geq 1$ drive the total reagents production towards meeting the demand; in this case, tests not performed because of lack of reagents are more likely due to poor resource allocation over the national territory, rather than an absolute scarcity of reagents. Under the bumpy pattern, for each factory we first choose two random days of the week $\tau_r^1, \tau_r^2 \in \{0, \dots, 6\}$, which we call “release days”. The factory will produce reagents at the same rate as under

Parameter	Description	Num values	Values
$ T $	Time horizon length	4	5, 7, 10, 14
$\lambda_{L \times R}$	Labs per region	3	5, 10, 20
$\lambda_{F \times R}$	Factories per region	4	0.1, 0.25, 0.5, 1
λ_{LC}	Lab capacity multiplier	7	0.5, 0.7, 0.9, 1, 1.1, 1.3, 1.5
λ_{LF}	Number of factories supplying each lab	3	1, 2, 3
λ_{LL}	Radius for inter-regional swab transfers	6	0, 5, 10, 15, 20, 25
λ_{FP}	Factory production multiplier	5	0.8, 0.9, 1, 1.1, 1.2
λ_{PP}	Factory production pattern	2	steady, bumpy

Table 2: Synthetic instance generation parameters.

ind. variable	% swabs tested		swab wait time	
	coef	p -value	coef	p -value
intercept	44.93	$< 10^{-3}$	0.36	$< 10^{-3}$
$ T $	0.84	$< 10^{-3}$	-0.13	$< 10^{-3}$
$\lambda_{L \times R}$	-0.69	$< 10^{-3}$	0.01	$< 10^{-3}$
$\lambda_{F \times R}$	4.07	$< 10^{-3}$	0.07	$< 10^{-3}$
λ_{LC}	5.56	$< 10^{-3}$	0.09	$< 10^{-3}$
λ_{LF}	3.19	$< 10^{-3}$	0.04	$< 10^{-3}$
λ_{LL}	0.54	$< 10^{-3}$	0.02	$< 10^{-3}$
λ_{FP}	0.70	$< 10^{-3}$	0.01	$< 10^{-3}$
λ_{PP}	-13.51	$< 10^{-3}$	-0.20	$< 10^{-3}$

Table 3: Results of a linear regression analysis using the instance generation parameters as independent variables and the primary (number of swabs tested, expressed as a percentage of the total demand) and secondary (average waiting time of a swab before it’s tested) objectives. Columns *coef* report the linear regression coefficients, after centring and standardising the inputs. All independent variables resulted significant, with p -values always smaller than 0.001.

the steady pattern, but won’t make them available until the current day t corresponds to one of the two τ_r^1, τ_r^2 (i.e., $t = 0 \bmod \tau_r^1$ or $t = 0 \bmod \tau_r^2$). At that point, it’s ready to ship all the reagents produced since the last release day. This second pattern simulates a situation in which it’s infeasible, due to logistic constraints, to have daily shipments out of the factories. Figure 7b shows an example of bumpy production. The coloured bars correspond to the quantities released by the factories on their release days, while grey background bars count the total amount of reagents released on that day, by all factories. The figure shows that, even if factories have, in principle, a steady production rate (only fluctuating between -5% and $+5\%$ due to the noise term ϵ), making new reagents available twice per week produces an uneven total daily distribution.

Table 2 summarises all instance generation parameters we used. Because in our scenario analysis we vary each parameter independently, we ran the Hierarchical Model over the full grid of 60 480 possible scenarios.

6.2.2 Scenario analysis

We report the results of our scenario analysis, highlighting how the instance generation parameters affect the testing capacity and commenting on which real-life decisions a planner can take to increase the number of swabs tested. A better testing capacity depends on both structural factors (such as a strong reagent industrial base) which require long-term decisions, and organisational factors (such as more inter-regional collaboration) which are influenced by operational decisions. Figure 8 shows how the percentage of swabs tested within the end of the time horizon changes, when varying each instance generation parameter. Each chart corresponds to one parameter; we used line charts for the seven numeric parameters, and a box plot for λ_{PP} , which is

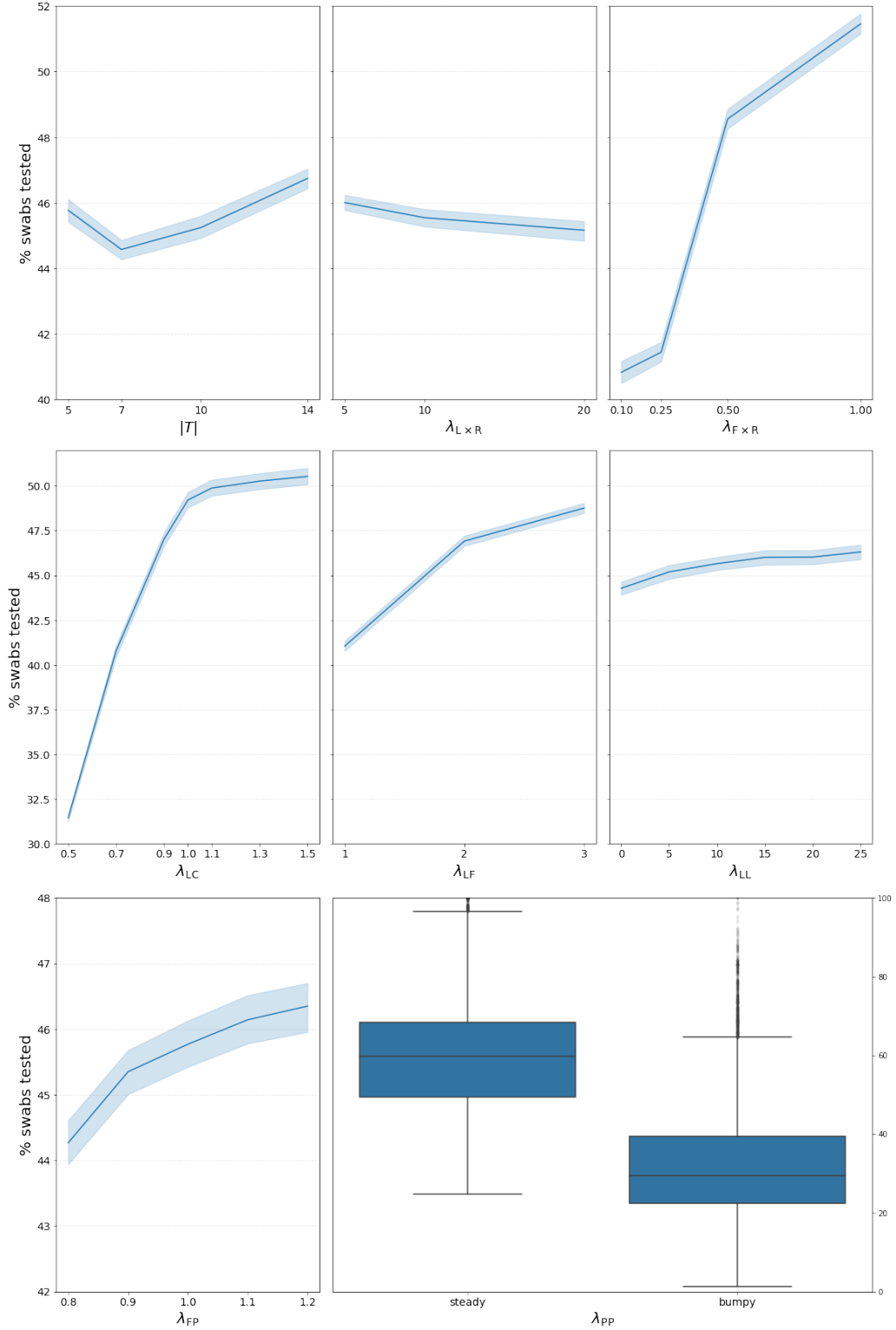


Figure 8: Variation in the percentage of swabs tested (y axis), when varying each instance generation parameter (x axis). In each chart, the line shows the average over all instances generated with the given parameter value and the shaded area around the line is the 95% confidence interval (obtained with 1000 bootstrap iterations). For parameter λ_{pp} , as it takes categorical values, we show a box plot instead of a line plot. The central line indicates the median, the box spans the two central quartiles, while whiskers extend to the rest of the distribution, except for outliers marked with fliers.

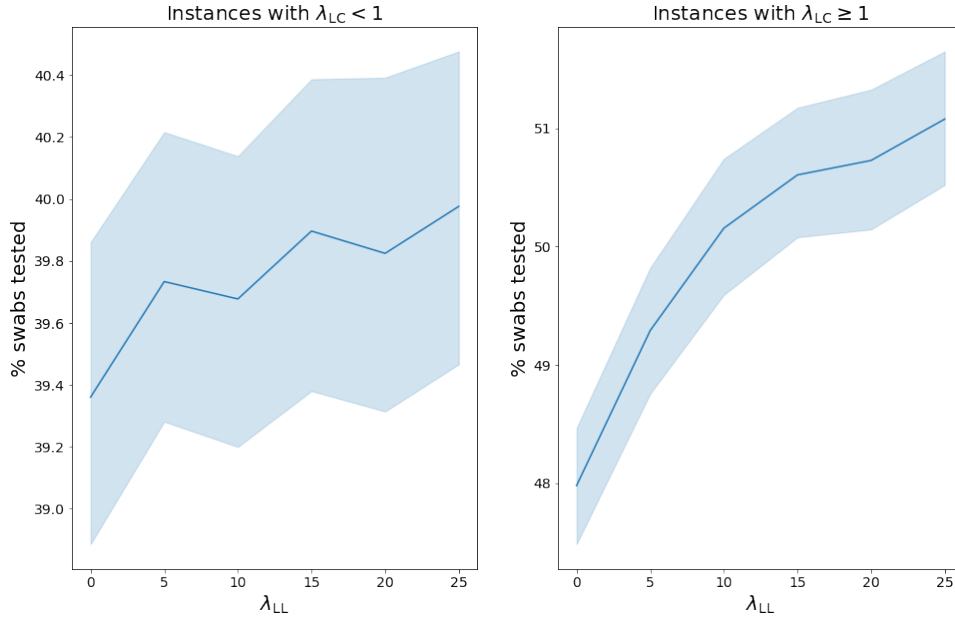


Figure 9: Variation in the percentage of swabs tested (y axis), when varying parameter λ_{LL} (x axis). The chart on the left refers to instances with $\lambda_{LC} < 1$, while that on the right, to instances with $\lambda_{LC} \geq 1$.

categorical. Two linear regression analyses provide additional findings. They use the instance parameters (after centring, standardising and transforming λ_{PP} into a numeric parameter, with value 0 if the production was steady and 1 if bumpy) as independent variables. The percentage of swabs tested and the average time a swab spent in a lab waiting to be tested are, respectively, the dependent variables in the two analyses. Table 3 reports the results, while in the following we comment on the insights obtained.

Steadiness of reagent supply. Parameter λ_{PP} is the one with the largest impact in our analysis: a steady availability of reagents allows the laboratories to operate without interruptions, testing more swabs and with shorter delays. The average percentage of swabs tested when $\lambda_{PP} = \text{steady}$ is double than when $\lambda_{PP} = \text{bumpy}$. Recall that a factory in our model can represent a real production site, but also a warehouse or a shipment from abroad. A physical factory will be able to maintain a steadier production rate, while relying on shipments will resemble more the “bumpy” scenario. The analysis, thus, hints to the fact that a solid industrial sector and a well-function supply chain can have the greatest impact on testing capacity; not necessarily because they allow to procure more reagent in total, but because they provide a steadier flow of it. A country that cannot count on such production capacity can mitigate the adverse effects of irregular supply with larger orders (see the positive impact of parameter λ_{FP}), more inventory capacity and a quick dispatch of reagents to labs.

Capillarity of the reagent industry. Having more small reagent production sites works better than having few, larger ones (parameter $\lambda_{F \times R}$). When $\lambda_{F \times R}$ moves from 0.1 to 1.0, the average percentage of swabs tested climbs from 40.83% to 51.46%. An efficient supply chain which is able to move material over longer distances (parameter λ_{LF}) also has a positive impact on testing capacity. When each lab can procure from its closest factory ($\lambda_{LF} = 1$), the analysis shows that 41.05% of swabs are tested. This number increases to 46.92% and then to 48.76%, when λ_{LF} increases to, respectively, 2 and 3.

Lab capacity and inter-regional capacity sharing. Other two factors which impact the amount of swabs tested are lab capacity and the degree to which regions can share this capacity by transferring swabs between each other. Parameter λ_{LC} clearly influences testing capabilities: for $\lambda_{LC} < 1$ largely less than half of the swabs are tested within the end of the time horizon. When $\lambda_{LC} \geq 1$, i.e., when the total lab capacity is at least as large as the average demand, gains are marginal, as exhibited by the curve flattening in Figure 8. It’s at this point that we would expect capacity sharing via increased inter-regional collaboration to have the greatest effect. The extent at which capacity is shared depends on parameter λ_{LL} . It might appear, looking at Figure 8, that the impact of λ_{LL} is small. However, if we divide the analysis of its impact between instances with $\lambda_{LC} < 1$

and instances with $\lambda_{LC} \geq 1$, the situation is different, as reported in Figure 9. Note how the curve referring to instances with $\lambda_{LC} \geq 1$ is much steeper, corresponding to a larger percentage increase in swabs tested. We can conclude that countries with insufficient lab infrastructures should primarily focus on procuring test machinery and training personnel to carry out rRT-PCR tests. Countries which already have a developed test lab network, on the other hand, benefit more from inter-regional collaboration and centralised planning than they do from increasing lab capacity.

Other factors. The percentage of swabs tested decreases when there are fewer, larger regions (parameter $\lambda_{L \times R}$). This is because, with fewer regions, the impact of one region being critical, i.e., with larger demands m_{it} , is proportionally larger. The effect of region size is rather modest, as indicated by a small regression coefficient associated with $\lambda_{L \times R}$. Regarding the planning horizon length $|T|$, its impact is unclear. On one hand, a longer time horizon allows more opportunities for optimisation. On the other hand, there is a reduction in tested swabs when moving from $|T| = 5$ to $|T| = 7$, which is hard to explain. In practice, a planner would want to balance the advantages usually conferred by longer-term planning with the quality of the demand predictions that he can obtain from epidemiological models. Finally, note that while the signs of the regression coefficients in the two regression analyses tend to coincide (meaning that parameters which have a positive impact on the number of swabs tested also have a positive impact on shortening wait times), the signs disagree for parameters $\lambda_{L \times R}$ and $|T|$, making it difficult to derive actionable recommendations for decision makers based on these two parameters.

7 Conclusions

We have proposed a model for the problem of assigning reagents and swabs to laboratories in a country which wants to maximise the number of rRT-PCR tests during a viral epidemic. After describing an Integer Programming model for a basic version of the problem, we have strengthened and extended the formulation to take into account real-life aspects of the organisation of healthcare systems. The complete model takes into account that many countries manage healthcare at a regional level, and allows to optimise two hierarchical objectives: primarily, maximising the number of tests performed and, secondarily, minimising the average time a swab waits before it's tested.

We performed two computational studies: the first based on real-life data from Italy and the second on synthetic instances. Under the assumptions we used, the main one being that reagents availability is often a bottleneck for testing more swabs (see, e.g., [12, 1, 41]), the analysis has revealed two main findings:

- Increased inter-regional coordination has the potential of increasing the testing capabilities of the country as a whole, as shown by the analysis of Italian data. In particular, moving swabs from critical regions to regions with spare capacity produced an increase of up to 40% in the number of swabs tested in the Italian scenario. The study performed on synthetic data confirmed this finding, but found a more modest effect. The recommendation, in fact, is that countries which don't have adequate lab infrastructure (i.e., which would have insufficient test capacity even if fully stocked with reagents) first focus on expanding their lab network, e.g., by purchasing new machines and training more lab personnel. Countries with an advanced laboratory infrastructure, instead, will benefit more from inter-regional collaboration.
- Steady availability of reagents has a large impact on the number of swabs tested and their waiting time. A solid chemical industrial base, with many (although possibly small) factories producing reagents daily gives an advantage compared with having to rely on a discontinuous supply, e.g., when purchasing from international markets.

On the short term, increasing inter-regional collaboration requires political will and an efficient supply chain which can be used to move swabs and reagents. On the other hand, increasing reagents production capacity involves longer-term investments and balancing the economic interests of pharmaceutical companies with national interests.

Future research on optimising the delivery of mass-scale test programmes can develop integrating other test types, such as immunological tests, i.e., tests which detect the presence of antibodies which a person has developed in response to the viral infection. These tests are too slow for early detection of positive patients;

e.g., T and B cells response to COVID-19 were detected around one week after the onset of symptoms [37], while swab tests can identify the virus even before symptoms appear. However, because antibodies persist in the blood even after a patient doesn't host the virus any longer, health authorities use immunological tests for mass-screening of populations (including asymptomatic patients) with the aim of assessing the prevalence of the virus, the level of population immunity and other epidemiological dynamics. It would be interesting to study not only how to increase capacity for immunological tests, but also to study the problem of selecting the patients to test with higher priority, in order to create an accurate epidemiological picture of the population while using a restricted supply of antibody tests such as ELISA (enzyme-linked immunosorbent assay) [39] or neutralization assays [43].

Acknowledgements

The author would like to thank Michele Iacono of Roche Diagnostics S.p.A. and Xavier Jiménez Fàbrega of the Health Department of Catalonia for comments and fruitful discussions on this work. The author was partially supported by grant "RTI2018-095197-B-I00" from the Spanish Ministry of Economy and Competitiveness.

References

- [1] Robert Baird. "Why Widespread Coronavirus Testing Isn't Coming Anytime Soon". In: *The New Yorker* (Mar. 24, 2020). URL: <https://www.newyorker.com/news/news-desk/why-widespread-coronavirus-testing-isnt-coming-anytime-soon>.
- [2] Aleksander Banasik, Argyris Kanellopoulos, Frits Claassen, Jacqueline Bloemhof-Ruwaard, and Jack van der Vorst. "Assessing alternative production options for eco-efficient food supply chains using multi-objective optimization". In: *Annals of Operations Research* 250.2 (2017), pp. 341–362. DOI: 10.1007/s10479-016-2199-z.
- [3] Pierre Bonami, Andrea Lodi, Andrea Tramontani, and Sven Wiese. "On mathematical programming with indicator constraints". In: *Mathematical programming* 151 (2015), pp. 191–223. DOI: 10.1007/s10107-015-0891-4.
- [4] Stephen Bustin. "Quantification of mRNA using real-time reverse transcription PCR (RT-PCR): trends and problems". In: *Journal of molecular endocrinology* 29 (1 2002), pp. 23–39. DOI: 10.1677/jme.0.0290023.
- [5] Hui Cao and Simin Huang. "Principles of scarce medical resource allocation in natural disaster relief: a simulation approach". In: *Medical Decision Making* 32.3 (2012), pp. 470–476. DOI: 10.1177/0272989X12437247.
- [6] Center for Disease Control and Prevention. *CDC 2019-Novel Coronavirus (2019-nCoV) Real-Time RT-PCR Diagnostic Panel*. Tech. rep. CDC-006-00019, Revision: 03. U.S. Department of Health and Human Services, Mar. 30, 2020. URL: <https://www.fda.gov/media/134922/download>.
- [7] Center for Disease Control and Prevention. *Processing of Sputum Specimens for Nucleic Acid Extraction*. Tech. rep. U.S. Department of Health and Human Services, Feb. 7, 2020. URL: <https://www.cdc.gov/coronavirus/2019-ncov/downloads/processing-sputum-specimens.pdf>.
- [8] Operations Research Center. *Optimization can solve the ventilator shortage*. 2020. URL: https://www.covidanalytics.io/ventilator_allocation.
- [9] Operations Research Center. *Ventilator Pooling: Formulation and Data Sources*. Tech. rep. Massachusetts Institute of Technology, 2020. URL: https://www.covidanalytics.io/ventilator_documentation_pdf.
- [10] Ye Chen, Linas Mockus, Seza Orcun, and Gintaras Reklaitis. "Simulation-optimization approach to clinical trial supply chain management with demand scenario forecast". In: *Computers & Chemical Engineering* 40 (2012), pp. 82–96. DOI: 10.1016/j.compchemeng.2012.01.007.
- [11] Covid19Italia. *Open Data Coronavirus*. 2020. URL: <https://www.covid19italia.info/opendata/>.
- [12] European Centre for Disease Prevention and Control. *Coronavirus disease 2019 (COVID-19) pandemic: increased transmission in the EU/EEA and the UK*. Tech. rep. Seventh update. Mar. 25, 2020. URL: <https://www.ecdc.europa.eu/sites/default/files/documents/RRA-seventh-update-Outbreak-of-coronavirus-disease-COVID-19.pdf>.
- [13] Adam Fleischhacker, Anh Ninh, and Yao Zhao. "Positioning Inventory in Clinical Trial Supply Chains". In: *Production and Operations Management* 24.6 (2015), pp. 991–1011. DOI: 10.1111/poms.12302.

- [14] George France, Francesco Taroni, and Andrea Donatini. “The Italian health-care system”. In: *Health Economics* 14 (S1 2005), S187–S202.
- [15] Willard Freeman, Stephen Walker, and Kent Vrana. “Quantitative RT-PCR: pitfalls and potential”. In: *Biotechniques* 26.1 (1999), pp. 112–125. DOI: 10.2144/99261rv01.
- [16] Nyoman Gunantara. “A review of multi-objective optimization: Methods and its applications”. In: *Cogent Engineering* 5.1 (2018). DOI: 10.1080/23311916.2018.1502242.
- [17] Gurobi Optimization LLC. *Gurobi Optimizer Reference Manual*. 2020. URL: <https://www.gurobi.com>.
- [18] Hsin-Chan Huang, Ozgur Araz, David Morton, Gregory Johnson, Paul Damien, Bruce Clements, and Lauren Ancel Meyers. “Stockpiling ventilators for influenza pandemics”. In: *Emerging Infectious Diseases* 23.6 (2017), pp. 914–921. DOI: 10.3201/eid2306.161417.
- [19] Deb Kalyanmoy. “Multi-Objective Optimization”. In: *Search Methodologies*. Ed. by Edmund Burke and Graham Kendall. 2014, pp. 403–449. DOI: 10.1007/978-1-4614-6940-7_15.
- [20] Neriman Beste Kaygisiz, Yashna Shivdasani, Rena Conti, and Ernst Berndt. *The Geography of Prescription Pharmaceuticals Supplied to the US: Levels, Trends and Implications*. Tech. rep. NBER Working Paper No. 26524. National Bureau of Economic Research, 2019. DOI: 10.3386/w26524.
- [21] Lorenzo Lampariello and Simone Sagratella. *Effectively managing diagnostic tests to monitor the COVID-19 outbreak in Italy*. Tech. rep. Optimization Online, 2020. URL: http://www.optimization-online.org/DB_FILE/2020/03/7680.pdf.
- [22] Sanjay Mehrotra, Hamed Rahimian, Masoud barah, Fengqiao Luo, and Schantz Karolina. *A Model of Supply-Chain Decisions for Resource Sharing withan Application to Ventilator Allocation to Combat COVID-19*. Tech. rep. Optimization Online, 2020. URL: http://www.optimization-online.org/DB_FILE/2020/04/7719.pdf.
- [23] Martin Meltzer, Anita Patel, Adebola Ajao, Scott Nystrom, and Lisa Koonin. “Estimates of the demand for mechanical ventilation in the United States during an influenza pandemic”. In: *Clinical Infectious Diseases* 60 (2015), S52–S57. DOI: 10.1093/cid/civ089.
- [24] Ministero della Sanità – Direzione Generale della Prevenzione Sanitaria. *Pandemia di COVID-19 – Aggiornamento delle indicazioni sui test diagnostici e sui criteri da adottare nella determinazione delle priorità. Aggiornamento delle indicazioni relative alla diagnosi di laboratorio*. Apr. 2020. URL: www.trovanorme.salute.gov.it/norme/renderNormsanPdf?anno=2020&codLeg=73799&parte=1%20&serie=null.
- [25] Mohammad Mirzapour Al-e-hashem, Hooman Malekly, and Mir Bahador Aryanezhad. “A multi-objective robust optimization model for multi-product multi-site aggregate production planning in a supply chain under uncertainty”. In: *International Journal of Production Economics* 134.1 (2011), pp. 28–42. DOI: 10.1016/j.ijpe.2011.01.027.
- [26] OpenToscana. *Open Data Covid19*. 2020. URL: <http://dati.toscana.it/dataset/open-data-covid19>.
- [27] Xingfei Pan, Dexiong Chen, Yong Xia, Xinwei Wu, Tangsheng Li, Xueting Ou, Liyang Zhou, and Jing Liu. “Asymptomatic cases in a family cluster with SARS-CoV-2 infection”. In: *The Lancet Infectious Diseases* 20.4 (2020), pp. 410–411. DOI: 10.1016/S1473-3099(20)30114-6.
- [28] Yves Pochet and Laurence Wolsey. *Production Planning by Mixed Integer Programming*. Operations Research and Financial Engineering. Springer, 2006. DOI: 10.1007/0-387-33477-7.
- [29] Francom Preparata and Michael Ian Shamos. *Computational Geometry: an Introduction*. Springer, 2012. DOI: 10.1007/978-1-4612-1098-6.
- [30] Presidenza del Consiglio dei Ministri – Dipartimento della Protezione Civile. *COVID-19 Italia: Monitoraggio della Situazione*. 2020. URL: <https://github.com/pcm-dpc/COVID-19>.
- [31] Steveb Sanche, Yen Ting Lin, Chonggang Xu, Ethan Romero-Severson, Nick Hengartner, and Rulan Ke. “High Contagiousness and Rapid Spread of Severe Acute Respiratory Syndrome Coronavirus 2.” In: *Emerging infectious diseases* 26.7 (2020). DOI: 10.3201/eid2607.200282.
- [32] Alberto Santini. *Increase COVID-19 Swab Testing Capacity via Optimisation*. 2020. URL: <https://santini.in/covid/>.
- [33] Alberto Santini. *Optimisation tools for the COVID-19 pandemic*. Github repository. May 4, 2020. DOI: 10.5281/zenodo.3785566. URL: <https://github.com/alberto-santini/covid-optimisation/>.
- [34] Ruggiero Seccia. *The Nurse Rostering Problem in COVID-19 emergency scenario*. Tech. rep. 2020. URL: http://www.optimization-online.org/DB_FILE/2020/03/7712.pdf.

- [35] Selma Souf. “Recent advances in diagnostic testing for viral infections”. In: *Bioscience Horizons* 9 (2016). doi: 10.1093/biohorizons/hzw010.
- [36] Task force COVID-19 del Dipartimento Malattie Infettive e Servizio di Informatica, Istituto Superiore di Sanità. *Epidemia COVID-19, Aggiornamento Nazionale*. Apr. 2020. URL: https://www.epicentro.iss.it/coronavirus/bollettino/Bollettino-sorveglianza-integrata-COVID-19_16-aprile-2020.pdf.
- [37] Matthew Zirui Tay, Chek Meng Poh, Laurent Réna, Paul MacAry, and Lisa Ng. “The trinity of COVID-19: immunity, inflammation and intervention”. In: *Nature Reviews Immunology* (2020). doi: 10.1038/s41577-020-0311-8.
- [38] Cheng Wang and Xiao-Bing Liu. “Integrated production planning and control: a multi-objective optimization model”. In: *Journal of Industrial Engineering and Management* 6.4 (2013), pp. 815–830. doi: 10.3926/jiem.771.
- [39] Yixuan Wang, Yuyi Wang, Yan Chen, and Qingsong Qin. “Unique epidemiological and clinical features of the emerging 2019 novel coronavirus pneumonia (COVID-19) implicate special control measures”. In: *Journal of Medical Virology* 92.6 (2020), pp. 568–576. doi: 10.1002/jmv.25748.
- [40] Janet Woodcock. *Safeguarding Pharmaceutical Supply Chains in a Global Economy*. 2019. URL: <https://www.fda.gov/news-events/congressional-testimony/safeguarding-pharmaceutical-supply-chains-global-economy-10302019>.
- [41] World Health Organisation. *Advice on the use of point-of-care immunodiagnostic tests for COVID-19*. Tech. rep. United Nations, Apr. 8, 2020. URL: <https://www.who.int/news-room/commentaries/detail/advice-on-the-use-of-point-of-care-immunodiagnostic-tests-for-covid-19>.
- [42] Di Wu, Tiantian Wu, Qun Liu, and Zhicong Yang. “The SARS-CoV-2 outbreak: what we know”. In: *International Journal of Infectious Diseases* (2020). doi: 10.1016/j.ijid.2020.03.004.
- [43] Fan Wu, Aojie Wang, Mei Liu, Qimin Wang, Jun Chen, Shuai Xia, Yun Ling, Yuling Zhang, Jingna Xun, Lu Lu, Shibo Jiang, Hongzhou Lu, Yumei Wen, and Jinghe Huang. “Neutralizing antibody responses to SARS-CoV-2 in a COVID-19 recovered patient cohort and their implications”. 2020.
- [44] Yisha Xiang and Jun Zhuang. “A medical resource allocation model for serving emergency victims with deteriorating health conditions”. In: *Annals of Operations Research* 236.1 (2016), pp. 177–196. doi: 10.1007/s10479-014-1716-1.
- [45] Stephanie Zaza, Lisa Koonin, Adebola Ajao, Scott Nystrom, Richard Branson, Anita Patel, Bruce Bray, and Michael Iademarco. “A conceptual framework for allocation of federally stockpiled ventilators during large-scale public health emergencies”. In: *Health security* 14.1 (2016). doi: 10.1089/hs.2015.0043.
- [46] Hui Zhao, Edward Huang, Runliang Dou, and Kan Wu. “A multi-objective production planning problem with the consideration of time and cost in clinical trials”. In: *Expert Systems with Applications* 124 (2019), pp. 25–38. doi: 10.1016/j.eswa.2019.01.038.

A Extended Model formulation

The extended model which incorporates the considerations made in [Section 4](#) uses a new variable $u_{lt} \in \mathbb{N}$, which represents the number of new swabs assigned to lab $l \in L$ on day $t \in T$. The model reads as follows:

$$\min \sum_{l \in L} z_{l|T|} \quad (22)$$

$$\text{s.t.} \quad \sum_{r \in R} \sum_{l \in L_i} x_{rlt} \leq q_i^{\text{rg}} \quad \forall i \in \{1, \dots, n\}, \forall t \in T \quad (23)$$

$$\sum_{l_1 \in L} \sum_{l_2 \in L_i} y_{l_1 l_2 t} \leq q_i^{\text{sw}} \quad \forall i \in \{1, \dots, n\}, \forall t \in T \quad (24)$$

$$x_{rlt} = 0 \quad \forall r \in R, \forall l \in L : \delta_{rl} = 0, \forall t \in T \quad (25)$$

$$y_{l_1 l_2 t} = 0 \quad \forall l_1, l_2 \in L : \mu_{l_1 l_2} = 0, \forall t \in T \quad (26)$$

$$z_{l,t-1} + u_{lt} + \sum_{\substack{l' \in L \\ \mu_{ll'}=1}} y_{l'l t} = z_{lt} + w_{lt} + \sum_{\substack{l' \in L \\ \mu_{ll'}=1}} y_{ll' t} \quad \forall l \in L, \forall t \in T \quad (27)$$

$$\sum_{l \in L_i} u_{lt} = m_{it} \quad \forall i \in \{1, \dots, n\}, \forall t \in T \quad (28)$$

$$w_{lt} \leq \rho_{l,t-1} + \sum_{\substack{r \in R \\ \delta_{rl}=1}} x_{rlt} \quad \forall l \in L, \forall t \in T \quad (29)$$

$$w_{lt} \leq Q_l \quad \forall l \in L, \forall t \in T \quad (30)$$

$$\rho_{r,t-1} + f_{rt} = \rho_{rt} + \sum_{\substack{l \in L \\ \delta_{rl}=1}} x_{rlt} \quad \forall r \in R, \forall t \in T \quad (31)$$

$$\rho_{l,t-1} + \sum_{\substack{r \in R \\ \delta_{rl}=1}} x_{rlt} = \rho_{lt} + w_{lt} \quad \forall l \in L, \forall t \in T \quad (32)$$

$$\gamma_{lt} = 0 \rightarrow w_{lt} \leq Q_l - 1 \quad \forall l \in L, \forall t \in T \quad (33)$$

$$\gamma_{lt} = 0 \rightarrow \rho_{lt} \geq 1 \quad \forall l \in L, \forall t \in T \quad (34)$$

$$\gamma_{lt} = 0 \rightarrow \sum_{\substack{l' \in L \\ \mu_{ll'}=1}} y_{ll' t} = 0 \quad \forall l \in L, t \in T \quad (35)$$

$$\gamma_{lt}^+ = 1 \rightarrow \sum_{\substack{l' \in L \\ l' \neq l}} y_{ll' t} \geq 1, \quad \gamma_{lt}^+ = 0 \rightarrow \sum_{\substack{l' \in L \\ l' \neq l}} y_{ll' t} = 0 \quad \forall l \in L, \forall t \in T \quad (36)$$

$$\gamma_{lt}^- = 1 \rightarrow \sum_{\substack{l' \in L \\ l' \neq l}} y_{l'l t} \geq 1, \quad \gamma_{lt}^- = 0 \rightarrow \sum_{\substack{l' \in L \\ l' \neq l}} y_{l'l t} = 0 \quad \forall l \in L, \forall t \in T \quad (37)$$

$$\gamma_{lt}^+ + \gamma_{lt}^- \leq 1 \quad \forall l \in L, \forall t \in T \quad (38)$$

$$x_{rlt} \in \mathbb{N} \quad \forall r \in R, \forall l \in L : \delta_{rl} = 1, \forall t \in T \quad (39)$$

$$y_{l_1 l_2 t} \in \mathbb{N} \quad \forall l_1 \in L, \forall l_2 \in L : \mu_{l_1 l_2} = 1, \forall t \in T \quad (40)$$

$$\rho_{rt} \in \mathbb{N} \quad \forall r \in R, \forall t \in T \quad (41)$$

$$\rho_{lt}, z_{lt}, w_{lt}, u_{lt} \in \mathbb{N} \quad \forall l \in L, \forall t \in T \quad (42)$$

$$\gamma_{lt} \in \{0, 1\} \quad \forall l \in L, \forall t \in T \quad (43)$$